Journal of Bioenergetics and Biomembranes, Vol. 37, No. 5, October 2005 (© 2005)
DOI: 10.1007/s10863-005-8642-5

ANT2 Isoform Required for Cancer Cell Glycolysis

Arnaud Chevrollier,[1] Dominique Loiseau,[1] Béatrice Chabi,[2] Gilles Renier,[1] Olivier Douay,[1] Yves Malthièry,[1] and Georges Stepien[3,4]

Received August 25, 2005; accepted September 26, 2005

The three adenine nucleotide translocator (ANT1 to ANT3) isoforms, differentially expressed in human cells, play a crucial role in cell bioenergetics by catalyzing ADP and ATP exchange across the mitochondrial inner membrane. In contrast to differentiated tissue cells, transformed cells, and their ρ^0 derivatives, i.e. cells deprived of mitochondrial DNA, sustain a high rate of glycolysis. We compared the expression pattern of ANT isoforms in several transformed human cell lines at different stages of the cell cycle. The level of ANT2 expression and glycolytic ATP production in these cell lines were in keeping with their metabolic background and their state of differentiation. The sensitivity of the mitochondrial inner membrane potential ($\Delta\psi$) to several inhibitors of glycolysis and oxidative phosphorylation confirmed this relationship. We propose a new model for ATP uptake in cancer cells implicating the ANT2 isoform, in conjunction with hexokinase II and the β subunit of mitochondrial ATP synthase, in the $\Delta\psi$ maintenance and in the aggressiveness of cancer cells.

KEY WORDS: Carcinogenesis; mitochondria; glycolysis; adenine nucleotide translocator.

INTRODUCTION

The mitochondrial adenine nucleotide translocator (ANT) catalyses ADP/ATP exchanges across the mitochondrial inner membrane. ANT plays an essential role in cell bioenergetics by regulating the ADP/ATP ratio in mitochondrial oxidative phosphorylation. In most eukaryotic organisms, ANT has three isoforms, each encoded by a distinct gene. Thus, yeasts have corresponding translocators, ADP/ATP carriers (AAC1 to AAC3) (Kolarov *et al*., 1990), and all mammals have ANT1 to ANT3 (Battini *et al*., 1987; Houldsworth and Attardi, 1988; Neckelmann *et al*., 1987), except for rodents in which only two isoforms (ANT1 and ANT2) have been identified (Graham *et al*., 1997; Levy *et al*., 2000).

ANT1 mRNA is specifically expressed in the heart, in skeletal muscle and to a lesser extent in the brain (Lunardi and Attardi, 1991; Stepien *et al*., 1992). *ANT2* expression is growth-dependent (Battini *et al*., 1987) and is a marker of cell proliferation (Barath *et al*., 1999). The *ANT2* gene is down-regulated in differentiating cell lines, but remains unexpressed, or only slightly expressed, in most tissues (Stepien *et al*., 1992). The human and bovine *ANT3* gene encodes an isoform expressed in all tissues in proportion to the mitochondrial oxidative phosphorylation (OXPHOS) content; its promoter region has the features of a housekeeping gene.

Both ANT1 and ANT3 export ATP produced by OXPHOS from the mitochondrial matrix to the cytosol. The overexpression of the ANT2 isoform in cells with a main glycolytic metabolism appeared puzzling (Stepien

[1] Inserm, U694, Angers, F-49033 France; Univ Angers, Angers, F-49035 France; CHRU Angers, Service d' Immunologie, Angers, F-49033 France.
[2] INRA, U1019, Clermont-Ferrand, F-63009 France; Univ Auvergne, Clermont-Ferrand, F-63001 France.
[3] Inserm U484, Clermont-Ferrand, F-63005 France; Univ Auvergne, Clermont-Ferrand, F-63001, France.
[4] To whom correspondence should be addressed at Inserm U484, BP 184, F-63005 Clermont-Ferrand CEDEX, France; e-mail: stepien@inserm484.u-clemontl.fr.

Key to abbreviations: $\Delta\psi$, mitochondrial internal membrane potential; ANT, adenine nucleotide translocator; ARP, acidic ribosomal phosphoprotein; ATPsynβ, β subunit of the Fl component of ATP synthase; $DiOC6_{(3)}$), 3,3′-dihexyloxacarbocyanine; 2-DOG, 2-deoxyglucose; HKII, hexokinase II; mClCCP, carbonyl cyanide m-chlorophenylhydrazone; mtDNA, mitochondrial DNA; ND4, NADH dehydrogenase 4; OXPHOS, oxidative phosphorylation; VDAC, voltage dependent anion channel.

et al., 1992). As suggested for the corresponding yeast *AAC3* isoform (Drgon *et al*., 1991), we hypothesized that *ANT2* had kinetic properties, different from those of the two other isoforms, allowing the uptake of glycolytic cytoplasmic ATP in exchange of intramitochondrial ADP. The survival in exclusive anaerobic conditions of a triple AAC yeast mutant, transformed with a human *ANT2* cDNA, reinforced this hypothesis (Giraud *et al*., 1998). The *ANT2* up-regulation is controlled by Sp1 (Zaid *et al*., 1999) and by an unidentified protein binding to the GRBOX promoter sequence (Giraud *et al*., 1998). The first seven nucleotides of the human GRBOX motif are present in the promoter sequences of the mouse *ANT2* gene (Levy *et al*., 2000) and the hypoxic consensus sequence present in the yeast *AAC3* gene (Balasubramanian *et al*., 1993). Moreover, the first six nucleotides of GRBOX are common to members of the SOX family associated with a DNA binding requirement (Pevny and Lovell-Badge, 1997).

In the present work, we have determined the respective roles of ANT2 and ANT3 in different cancer cell lines in relation to their metabolic status. Real-time quantitative RT-PCR allowed us to quantify, for the first time, the transcript copy number of each ANT isoform in cancer cells as compared to cultured untransformed cells and tissues. We show that the expression of ANT isoforms in cancer cells is closely related to the metabolic properties, cell cycle events, and maintenance of the $\Delta\psi$ of the mitochondrial membrane. The understanding of the specific ANT2 involvement in cancer cell proliferation should help to design new anti-tumor strategies targeting the *ANT2* transcript.

MATERIALS AND METHODS

143B $_{TK}$-(ATCC CRL 8303) is a human osteosarcoma cell line cultured in DMEM/F12 medium with 10% FCS (fetal calf serum) supplemented with penicillin G (100 μg/mL), streptomycin (100 μg/mL), and amphoptericin B (0.25 μg/mL). HepG2 is a hepatocarcinoma cell line (ATCC HB 8065) cultured in RPMI 1640 medium supplemented with FCS and antibiotics, at the same concentrations as those used for 143B cells. The ρ^0 HepG2 cell line was obtained by treatment of parental HepG2 cells with ethidium bromide for 7 weeks and selection of cells with complete mitochondrial DNA (mtDNA) depletion (Loiseau *et al*., 2002). The ρ^0 143B cell line was kindly provided by Dr. R. Morais (Montreal, Canada). Both ρ^0 cell lines, auxotrophic for uridine and pyruvate, were cultured in media identical to that of the corresponding parental cells, except for a supplement of uridine (50 μg/mL) and pyruvate (100 μg/mL). The WI38 cell line (human lung fibroblasts, ATCC MD CCL 75) was maintained in DMEM supplemented with 10% FCS, non essential amino-acids and antibiotics. Media were supplied by Gibco-BRL, FCS by Seromed (Biochrom, KG, Berlin Germany). All other chemicals were purchased from Sigma Chemical Co (St Louis, MO, USA). Cell proliferation was quantified during 7 days by direct cell counting every 24 h, in three different preparations. Doubling time (DT) was calculated from the exponential growth period as follows: DT $= (T2 - T1)$/[ln (cell number at T2/cell number at T1)/ln (2)], where $(T2 - T1)$ is the duration of the exponential phase.

The cell cycle was analyzed with a fluorescence-activated cell sorter (Becton Dickinson, San Jose, CA, USA). For flow cytometry, cells were fixed in 70% ethanol and DNA-Prep COULTER® reagent Kit (Beckman Coulter Inc., Fullerton, CA, USA). CellQuest (Becton Dickinson, San Jose, CA, USA) and ModFit 5.2 software (Verity Software House, Topsham, ME, USA) were used to analyze nuclear DNA distribution.

Glucose and lactate concentrations in the culture media were determined by spectrophotometry (Trinder, 1969), using appropriate enzymatic kits (Boehringer, Mannheim, Germany) on a Hitachi-Roche 917 apparatus (Roche Diagnostics GmbH, Mannheim, Germany). Data were expressed in terms of glucose consumption and lactate production and were normalized to total cellular protein content, as determined by the BC Assay kit (Uptima, Interchim, Monthuçon, France). Citrate synthase was assayed by spectrophotometry from whole cell homogenates (Shepherd and Garland, 1969). For ATP synthase activity, cells were harvested by trypsinisation. 1 and 2×10^6 cells were incubated in 200 μL of medium with either oligomycin (10 μM), or 2-deoxyglucose (2-DOG) (50 μg/mL) (Sigma, St Louis, MO, USA), for 20 min at 37°C. Cells were homogenized in 800 μL PBS and boiled for 5 min to inactivate cytoplasmic ATPases. The cell extract was immediately pelleted by centrifugation at $10,000 \times g$ at 4°C for 5 min and stored at −70°C. ATP concentration in samples was then determined using the Enliten® ATP Assay system Luciferase/Luciferin (Promega®, Madison, WI, USA) and a Minilumat Luminometer (Berthold Technologic, Bad Wilbad, Germany).

Total RNA was extracted from cultured cells using the RNeasy® Kit and the RNase-Free DNase set (Qiagen GmbH, Hilden, Germany) which provides efficient on-column digestion of nuclear and mtDNA during RNA purification. RNA concentration and integrity were assessed using an Agilent 2100 Bioanalyser (Agilent Technologies®, Waldbronn, Germany). First-strand cDNA synthesis was performed in duplicate using Superscript II reverse polymerase for RT-PCR on 1 μg

total RNA samples (dT) 15 primer (Invitrogen™, Carlsbad, CA, USA) as indicated by the manufacturer, and dNTPs (Gene AMP®dNTP Perkin Elmer, Boston, MA, USA) in a total of 20 μL.

The relative transcript levels were determined using real-time RT-PCR, with a LightCycler™ (Roche Molecular Biochemicals, Mannheim, Germany). At the end of the PCR cycles, melting curve analysis was performed according to LighCycler™ kit instructions, to assess the purity of PCR products. Amplified fragments were electrophoresed on agarose gels to confirm their expected sizes and were sequenced. Their identity was verified by sequence comparison to the Genbank database. Real-time PCR was performed according to the instructions in the LightCycler™ FastStart DNA Master SYBRGreen I Kit (Roche Diagnostics, Mannheim, Germany), using gene specific PCR forward (for)/reverse (rev) primers: *ANT2* (GCTTGTCTTGTATGATGAAA/AGAAAACTGGTCAGATGAAT); *ANT3* (TCGAGAAATTCCAGTTGTCTTT/AGAACACGACTTGGCTCCTACA); *ARP* (acidic ribosomal phos-phoprotein) (CG ACCTGGAAGTCCAACTAC/ATCTGCTGCATCTGCTTG); *ND4* (NADH dehydrogenase 4) (CATTACGATGTTGCCCG/GCGAGGTTAGCGAGGCTTGC); *HK II* (TCGCATCTGCTTGCCTACTTC/CTTCTGGAGCCCATTGTCCGT). Standards for all the cDNA fragments were cloned in pCR®2.1-TOPO vectors (Invitrogen™, Carlsbad, CA, USA) to assure higher stability. The relative levels of *ARP* mRNA were used as the internal standard. All copy number determinations were done with the LightCycler™ 'Fit Point Method' software.

Immunological analysis was performed as followed: cells grown in 15-cm diameter plates were rinsed in PBS, trypsinised, and collected in centrifuge tubes. The pellet was resuspended in 1 mL of water containing protease inhibitor cocktail (Complete™ tablets, Roche Diagnostics, Mannheim, Germany). SDS-PAGE gel electrophoresis was performed in 12.5% acrylamide gels. After electrophoresis, the proteins were dry-transferred to polyvinylidene difluoride membranes using an Owl™ apparatus. The membranes were incubated with dilutions of the following antibodies: polyclonal anti-ANT2 (Giraud *et al*., 1998), mouse IgG1 anti-α-tubulin (Sigma), monoclonal mouse IgG_{2b} anti-porin (Invitogen), and anti-cytochrome oxidase II (COX II) (Dr. A. Lombes, Institut de Myologie, Paris, France), in Tris buffered saline containing 0.05% Tween 20 (TBS-T) overnight at 4°C. After several washes in TBS-T, the membranes were incubated with an appropriate chemiluminescent-labeled horseradish peroxidase-conjugated secondary antibody (Jackson Immuno Research, WestGrove, PE, USA) (ECL™ Amersham Pharmacia Biotech western-blotting detection reagents, Buckinghamshire, UK). Signal quantification was performed by non-saturating picture scanning by a Gel Doc 1000 Molecular Analyst™ apparatus (Biorad, Hercules, CA, USA).

The mitochondrial internal membrane potential ($\Delta\psi$) was quantified as followed: cells were grown for 72 h, trypsinised, washed in PBS/5% FCS, and plated in 96-well plates (10^5 cells/100 μL/well). Cells were incubated in PBS/50 mM KCl/5% FCS containing the cationic fluorescent dye 3,3′-dihexyloxacarbocyanine ($DiOC6_{(3)}$) (20 nM) for 30 min at 37°C. To investigate the dependence of mitochondrial $\Delta\psi$ on mitochondrial or glycolytic ATP production, parallel incubations were performed in the presence of either OXPHOS inhibitors (5 μg/mL oligomycin, 5 μg/mL antimycin A, 30 μM aurovertin, 10 μM bongkrekic acid) or glycolytic inhibitors (100 μg/mL 2-deoxyglucose, 1 μM capsaicin). Ten μM of the mitochondrial uncoupler mClCCP (carbonyl cyanide m-chlorophenylhydrazone) was added to determine the residual fluorescence intensity when the mitochondrial $\Delta\psi$ collapsed. The integrity of the cell membrane was determined by 5 μg/mL propidium iodide. Fluorescence was analyzed on a FACScan flow cytometer (Becton Dickinson, San Jose, CA, USA), using CellQuest as software. All inhibitors were purchased from Sigma.

The results were analyzed (ANOVA) using StatView® (version 5.0). Differences between means, evaluated by Scheffe's *F*-test, were considered significant at $p < 0.05$.

RESULTS

ANT2 and ANT3 Expression in Cancer Cell Lines

To investigate the kinetic properties of ANT isoforms in cancer cells, we first quantified the *ANT* transcript levels in two cell lines: 143B osteosarcoma and HepG2 hepatocarcinoma cell lines. After reverse transcription, real-time quantitative PCR allowed the precise determination of the cDNA copy number. When the *ANT* transcript copy number was normalized to that of *ARP* selected as standard (Fig. 1), the expression of *ANT2* was about ten times greater than that of *ANT3* in 143B cells, whereas the expression of *ANT3* was twice that of *ANT2* in HepG2 cells. Moreover, when these *ANT2* levels in 143B and HepG2 cells were compared to those in untransformed WI38 fibroblasts or myoblasts, the higher level of *ANT2* expression in cancer cell lines (up to 13-fold) was confirmed. Finally, the expression of *ANT2* in 143B cells was up to 100 times greater than that in skeletal muscle (Fig. 1), and liver (data not shown). *ANT* expression in

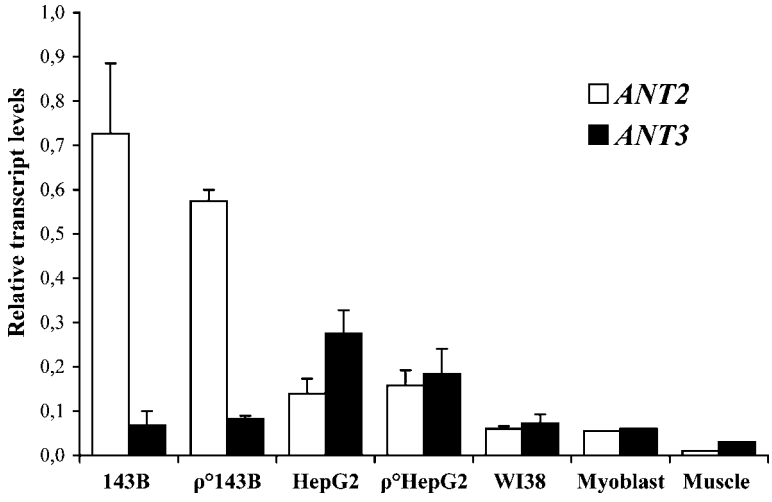

Fig. 1. Levels of *ANT2* and *ANT3* transcripts in 143B, HepG2 cells, the corresponding ρ^0 cells, untransformed cells, and skeletal muscle. The histograms represent the values determined by quantitative real-time RT-PCR (RNA was extracted from cells harvested under the same exponential growth conditions). For each sample, the RT-PCR results were normalized to the control *ARP* transcript level (results are means of at least three samples ±S.D.).

the corresponding 143B and HepG2 ρ^0 cells (mtDNA-depleted cells) followed a similar pattern, confirming the glycolytic status of both ρ^0 and parental transformed cells.

ANT expression was quantified at the protein level by Western blotting. Total protein extracted from the same cell lines was immuno-detected with a polyclonal antibody directed to the ten *N*-terminal amino acids of the ANT2 isoform (Fig. 2). The mitochondrial content of each cell line was evaluated by quantification of either porin, nuclear encoded mitochondrial protein of the Voltage Dependent Anion Channel (VDAC) complex, or COX II, an mtDNA encoded mitochondrial protein. Assuming that the regulation of *ANT* expression occurs predominantly in the transcriptional step, the ANT2 protein levels, normalized to the standard α-tubulin, confirmed the over-expression of the *ANT2* transcript (Fig. 1).

Interaction of *ANT* Expression with that of Other Genes Involved in Metabolic Pathways

The ANT protein could be thought of as being at the crossroads between glycolysis and OXPHOS. Hexokinase II (HK II), a glycolytic enzyme that binds to mitochondria, was found to be highly expressed in 143B and ρ^0 143B cells as compared to the control untransformed WI38 fibroblasts (Fig. 3). ATPsynβ, a subunit of the hydrophilic F1 component of ATP synthase, was also highly expressed in 143B cells. Mitochondrial *ND4* gene expression was higher in HepG2 than in 143B and WI38 cells, the expression pattern following that of the *ANT3* gene (Fig. 1). The complete absence of *ND4* expression in 143B and HepG2 ρ^0 cells, even after multiple passages,

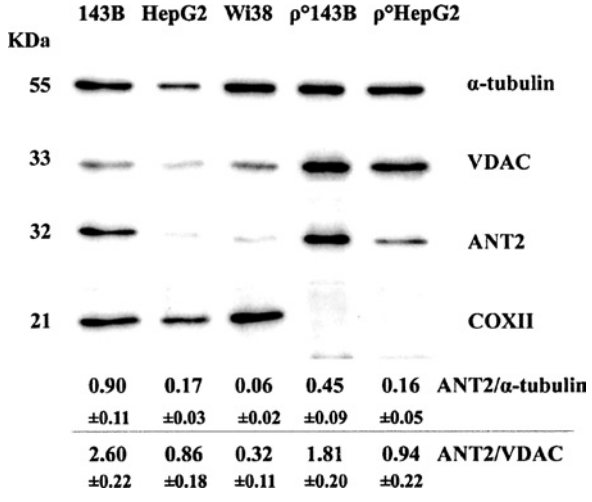

Fig. 2. Comparison of ANT2 protein levels in 143B, HepG2, the corresponding ρ^0 cells, and WI38 fibroblasts. Immunoblot of whole cell extracts probed with antibodies against ANT2 (polyclonal *N*-terminal ANT2), mitochondrial-encoded cytochrome *c* oxidase subunit 2 (monoclonal COX II), the cytoplasmic α-tubulin (polyclonal), and mitochondrial nuclear encoded porin. The protein weights are indicated to the left. The relative ANT2 to α-tubulin protein levels are indicated under each lane (results are means ± S.D., $n = 4$).

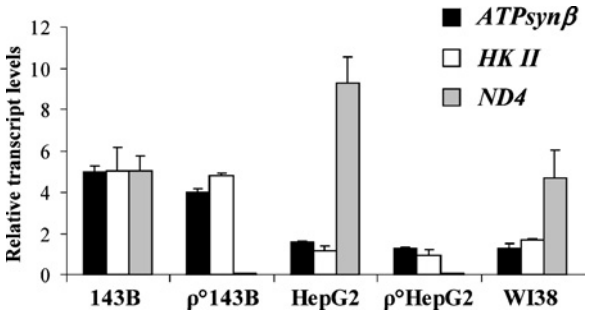

Fig. 3. Transcript levels of genes involved in energy metabolism in 143B, HepG2, the corresponding ρ^0 cells, and WI38 fibroblasts. The histograms represent relative RNA levels determined by real-time quantitative RT-PCR. For each sample, the RT-PCR results were normalized to the control *ARP* transcript level. Values were normalized to the 143B ATPsynβ/ARP ratio (HKII/ARP ratios multiplied by five and ND4/ARP ratios divided by 50). (Results are means of at least three different determinations (±S.D.).

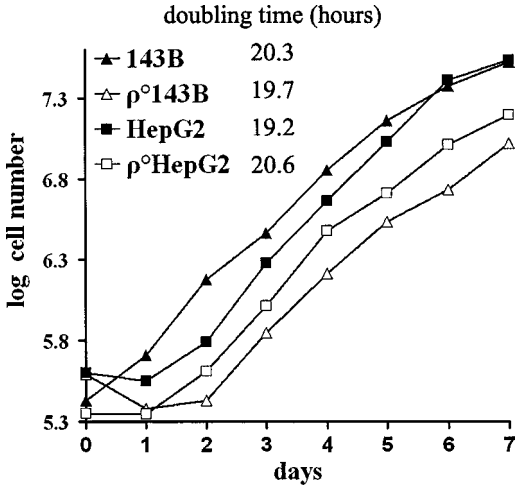

Fig. 4. Proliferation of 143B, HepG2, and corresponding ρ^0 cells. Increase in cell number was analyzed by direct cell counting every 24 h for 7 days in three different preparations. Corresponding doubling times are indicated.

confirmed the total and permanent mtDNA depletion in these cell lines.

Glycolytic Metabolism of Transformed Cells

The metabolic status of the cell lines was characterized by the quantification of both lactate and glucose in the culture medium. Lactate production and glucose oxidation were higher in 143B than in HepG2 cells (Table I), indicating higher glycolytic activity in 143B cells. However, these results concerned the first 24 h of the growth kinetic, i.e. before the cells had reached their exponential phase. HepG2 cells needed more time (about 48 h) than 143B cells to display complete glycolytic activity (Fig. 4). After this 24–48 h latency period, the doubling time was the same in 143B, HepG2, and corresponding ρ^0 cells, suggesting that the global cell cycle time was similar in all cell lines.

At optimal concentrations, oligomycin (an inhibitor of mitochondrial ATP synthase) or 2-deoxyglucose (2-DOG) (an inhibitor of glycolysis) induce the total inhibition of mitochondrial (oligomycin) and cytoplasmic (2-DOG) ATP synthesis, leading to cell death (Kaplan, 2001). To test the sensitivity of each cell line, we used oligomycin and 2-DOG with limited time exposures (20 min). In the presence of oligomycin (Table I), whole-cell ATP levels decreased, attesting to mitochondrial ATP production both in HepG2 and 143B cells in the first 24 h of culture. As previously reported (Jouaville *et al.*, 1999), the treatment of transformed cells with oligomycin did not significantly modify the ATP pattern, showing that glycolysis is the main metabolic pathway in these cells.

Table I. Biochemical Characterization of 143B, HepG2, and Corresponding ρ^0 Cells

	Glucose oxidation (mmol/24 h/mg)	Lactate production (mmol/24 h/mg)	ATP levels +oligomycin (% of control)	ATP levels +2-DOG (% of control)	Citrate synthase activity (U/mg prot)
143B	4.27 ± 0.27	7.54 ± 0.31	65.1 ± 5.2	61.5 ± 4.4	181±7
ρ^0 143B	6.11 ± 1.44	9.12 ± 0.63	n.d.	n.d.	165 ± 11
HepG2	2.22 ± 0.16	3.18 ± 0.31	53.8 ± 6.3	82.6 ± 2.8	306 ± 32
ρ^0 HepG2	3.83 ± 0.33	5.62 ± 0.29	n.d.	n.d.	257 ± 32

Note. Glucose oxidation, lactate production, ATP levels, and citrate synthase activity were determined in 143B and HepG2 cells (means ± S.D., $n = 3$–4). Glucose consumption and lactate production were determined in culture media 24 h following medium change and expressed relative to the cellular protein content. ATP levels represent cellular ATP content following a 20 min inhibitor treatment and are given as percentage of ATP levels in cells without inhibitors (oligomycin: mitochondrial ATP synthase inhibitor; 2-DOG: glycolysis inhibitor). Citrate synthase activity was measured in total cell extract, n.d.: not determined.

In contrast, the effect of the glycolysis inhibitor 2-DOG was greater in 143B than in HepG2 cells, indicating an early involvement of glycolysis in the growth kinetics of 143B cells.

Changes in Energetic Metabolism During the Cell Cycle

Forty-eight hours of serum starvation (without FCS) of WI38, 143B, and HepG2 cells induced cell cycle arrest and produced a homogeneous population, with more than 90% of the cells in the GO/G1 phase. Passage in a fresh medium containing serum induced cell cycle progression. The W138, 143B, and HepG2 cells, which attained maximal DNA synthesis 21, 23, and 24 h later respectively as shown by flow cytometry analysis, were mostly in the S phase. To study the G1/S transition, cells were harvested in each of the phases. *ANT2* overexpression has been related to serum induction (Giraud *et al*., 1998) and the exponential growth phase (Lunardi and Attardi, 1991). Our results showed specific *ANT2* overexpression (up to 60%) in all tested cells during the Gl/S transition (Table II). The marked upregulation of *ANT2* in WI38 cells is explained by the low G0/G1 expression level of *ANT2* in untransformed cells as compared to the 143B and HepG2 cells (Fig. 1). HK II (glycolytic enzyme) and ATPsynβ (from the oxidative ATP synthase complex) were simultaneously induced, up to 90 and 70% respectively, in 143B cells. 143B cells were the only cells able to maintain their mitochondrial gene expression during the G1/S transition.

Table II. Expression of Genes Involved in Energy Metabolism During G1/S Transition

	% of mRNA copy number (S versus G0/G1 phase)		
	143B	HepG2	WI38
ANT2	126 ± 7	121 ± 3	162 ± 5
ANT3	100 ± 3	83 ± 3	103 ± 5
HK II	189 ± 12	92 ± 3	92 ± 5
ATPsynβ	169 ± 8	102 ± 12	110 ± 8
ND4	113 ± 4	50 ± 5	61 ± 2

Note. Total RNA was extracted from synchronized cells in the G0/G1 and S phases (Fig. 4). After reverse transcription, the *ANT2*, *ANT3*, *HK II*, *ATPsynβ* , and *ND4* mRNA copy numbers were determined by real-time quantitative PCR. cDNA copy numbers were normalized to the control *ARP* gene copy number. Results represent ratios of relative transcript levels in the S versus the G0/G1 phases, expressed as percentages. The significantly upregulated genes are indicated with a grey background. Results express the means of at least three different preparations (±S.E.M.).

Mitochondrial *ND4* expression in HepG2 and WI38 cells was reduced by 50 and 39%, respectively. However, the citrate synthase enzymatic activity was constant in whole cell extracts (not shown), suggesting that the mitochondrial mass had not increased during this phase. These results showed that mitochondrial gene expression was not synchronized with cell cycle progression.

Effects of OXPHOS and Glycolysis Inhibitors on the Mitochondrial $\Delta\psi$ of Transformed Cells

The fluorescence from the DiOC6(3) dye in the HepG2, 143B, and corresponding ρ^0 cells was decreased by about 60% after treatment with the uncoupler mClCCP. This corresponds to the collapse of the mitochondrial membrane $\Delta\psi$. Residual fluorescence was chosen as the base line (Fig. 5). Even if fluorescence signals cannot be directly related to membrane potential values, the almost all-or-none variations observed with the different inhibitors could lead to the following observations: The full OXPHOS inhibition by the respiratory chain inhibitor antimycin and by the ATP synthase inhibitor oligomycin caused the HepG2 $\Delta\psi$ to collapse, indicating that HepG2 cells, out of their exponential growth phase, rely mainly on oxidative metabolism in such culture conditions. This was confirmed by (i) the weak effect of glycolysis inhibitors (2-DOG or capsaicin); and ii) by the absence of any effect of either aurovertin or bongkrekic acid on the inhibition of the ATP/ADP exchange since proton ejection by the respiratory chain could by itself maintain the $\Delta\psi$. In contrast, all these inhibitors of OXPHOS and glycolysis showed a partial effect on the $\Delta\psi$ in 143B cells, suggesting a dual oxidative/glycolytic metabolism. The collapse of the $\Delta\psi$ caused by ANT inhibitors indicated that glycolysis was predominant in such cells. Finally, the full collapse of the $\Delta\psi$ by glycolysis inhibitors in the two ρ^0 cells, together with the absence of effects of OXPHOS inhibitors, confirmed their exclusive glycolytic metabolism.

DISCUSSION

Glycolysis and Mitochondrial Activity in Transformed and ρ^0 Cells

The question of impaired mitochondrial function in cancer cells was first raised almost fifty years ago (Warburg, 1956). A glycolytic phenotype has now been confirmed at the biochemical as well as the molecular level in cancer cells. All mitochondrial genes were found to be down-regulated in tumor biopsies and cancer cell lines as compared to controls (Faure Vigny *et al*., 1996).

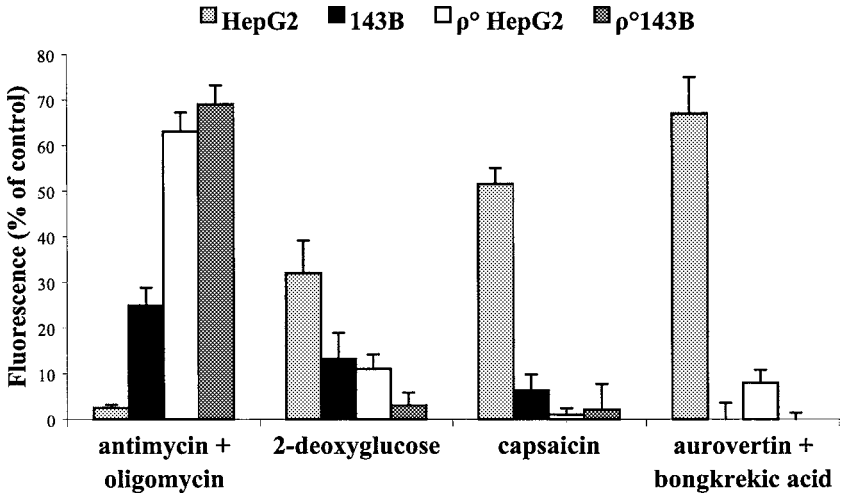

Fig. 5. Effect of OXPHOS and glycolysis inhibitors on the $\Delta\psi$ of HepG2, 143B, and ρ^0 cells. Cells (10^5/100 μl) incubated in PBS/50 mM KCL/5% FCS containing 20 nM DiOC6(3) were treated with either 10 μM mClCCP or mitochondrial inhibitors (5 μg/mL oligomycin, 5 μg/mL antimycin A, 30 μM aurovertin, 10 μM bongkrekic acid) or glycolytic inhibitors (100 μg/mL 2-deoxyglucose, 1 μM capsaicin) for 30 min at 37°C. Inhibitors were added together where indicated. After subtraction of residual values from mClCCP treated cells, data are expressed as percentages of fluorescence intensity from untreated cells.

These results were supported by the observed decrease of cellular mitochondrial content in various tumors (Cuezva *et al.*, 2002). The nuclear and mitochondrial DNA replication and transcription processes are not coupled and this should lead to a lowered mtDNA/nuclear DNA ratio as a consequence of the high cell growth and division. However, despite the neoplasic transformation, the mitochondrial content in a cell may be more linked to the original tissue properties than a common pathway of regulation.

Because of the absence of mtDNA-encoded proteins, there is no OXPHOS activity in ρ^0 cells so that the exclusive source of ATP is glycolysis. Thus, when compared to cells with functional mitochondria, ρ^0 cells may be expected to be more sensitive to glycolytic inhibitors since they are unable to switch to an alternative oxidative metabolism. It has been shown that ρ^0 143B cells are 10 times more sensitive to 2-deoxyglucose than wild type 143B cells (Liu *et al.*, 2001). In our study, complete glucose privation led to the death of all ρ^0 cells, whereas it was possible to maintain parental cells in culture, although with a very low division rate (data not shown). In ρ^0 cells, the synthesis of enzymes involved in mitochondrial functions is not reduced. Nevertheless, the lack of the 13 mtDNA-encoded proteins leads to disorganization of the cristae without local alteration of the inner membrane. Nuclear *OXPHOS* gene expression was shown to be unaffected in ρ^0 cells despite the absence of mtDNA (Duborjal *et al.*, 2002). No clear feedback phenomenon was induced to correct for the defect of mitochondrial ATP production.

ANT Isoforms in Cancer Cells

The kinetic properties of the ANT1 and ANT3 isoforms allow ATP export from mitochondria in cells with an oxidative metabolism. We previously hypothesized that the ANT2 isoform might be specifically expressed to import glycolytic ATP when the mitochondrial OXPHOS activity switched to a glycolytic metabolism (Stepien *et al.*, 1992). The present study confirms that the *ANT2* and *ANT3* genes are co-expressed in tumor cells as well as in untransformed cells. Whereas the *ANT3* gene is expressed in all cells and tissues, *ANT2* expression is upregulated in transformed cells. Indeed, there is a 10-fold increase in the 143B cell line as compared to untransformed cells, and a 50-fold increase compared to muscle tissue. Moreover, *ANT2* overexpression differed in the two transformed cell lines studied and this variation was unrelated to a rate difference in growth and division. The comparison between transformed cells with mtDNA (143B, HepG2) or without mtDNA (ρ^0 143B, ρ^0 HepG2) showed similar *ANT2* overexpression. Our polarographic studies (data not

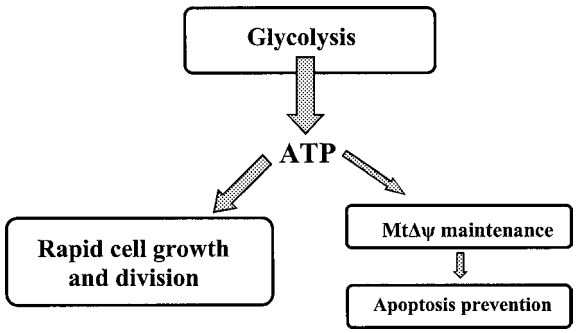

Fig. 6. Glycolytic ATP requirements in cancer cells. Most of the glycolytic ATP is required by the anabolism pathways of rapidly growing cells and a part is imported into mitochondria through HK II, VDAC, and ANT2 to maintain the $\Delta\psi$ of mitochondrial internal membrane and the intramitochondrial metabolic pathways.

shown), as well as those by other authors (Villani *et al*., 1998), showed that the *in vitro* oxygen consumption, and consequently the OXPHOS content, of HepG2 cells is higher than that of 143B cells. These results suggest that transformed HepG2 cells retain some properties of differentiated liver cells. In the liver, the ANT protein content was shown to be lower than in other tissues (Kunz, 2003) and this may explain why ATP export was so low even though hepatic cells normally maintain the active mitochondrial ATP production required for liver-specific intra-mitochondrial metabolic pathways such as the urea cycle and gluconeogenesis (Groen *et al*., 1982).

ANT Expression and the Cell Cycle

Few studies have linked the cell cycle to mitochondrial ATP synthesis. The serum induction of glycolytic enzymes, observed in the first step of the G1/S transition, suggested the predominance of glycolytic pathways in dividing cells (Netzker *et al*., 1994). *ANT2* is upregulated during the Gl/S transition in tumor cells and the simultaneous induction of *HK II* could be linked with glycolytic gene expression in the early G1 phase (Burger *et al*., 1994; Marjanovic *et al*., 1991). Our results showed an increase of *ATPsynβ* gene expression in the G1/S transition stage. Other ATP synthase subunits such as 5A1 were found to be overexpressed in ρ^0 cells from a breast cancer cell line (Delsite *et al*., 2002). The overexpression of ATP synthase subunits in cancer cells could be directly related to the maintenance of the $\Delta\psi$. The hydrolysis of imported glycolytic ATP^{4-} by the F1 component of ATP synthase leads to (i) ADP^{3-} release from mitochondria with the gain of a negative charge on the matrix side; and (ii) proton ejection towards the intermembrane space through the F0 component (Fig. 7).

ANT2 and Glycolytic ATP Import in Mitochondria

The induction of ANT2 expression in cancer cells is directly related to their glycolytic metabolism. Cancer cells present a switch to a predominant glycolytic metabolism leading to cellular accumulation of intermediates such as lactate. This incomplete oxidation provides a proliferative advantage because of the availability of such intermediates for active cell anabolism. Thus, ANT2 should have kinetic parameters favoring glycolytic ATP uptake into mitochondria, required for the maintenance of the mitochondrial $\Delta\psi$ (Buchet and Godinot, 1998) and specific intra-mitochondrial anabolic pathways, essential for eukaryotic cell growth. The produced ADP would then exit mitochondria from ANT2 and be re-phosphorylated via the downstream reactions of glycolysis. Moreover, this ATP uptake could shut down mitochondrial OXPHOS either by controlling the ATP/ADP ratio or by direct binding to subunits of the cytochrome oxidase complex (Lee *et al*., 2002). As indicated by their doubling times, wild type and ρ^0 cells without functional OXPHOS have the same growth rate, confirming that glycolytic ATP production is the major energy source during the cell growth and division (Fig. 6). Previous results showed that overexpression of both *ANT1* in human embryonic cells (Bauer *et al*., 1999) and *ANT3* in HeLa cells (Zamora *et al*., 2004) induces apoptosis. Such an increase of the mitochondrial ATP to cytosolic ADP exchange by these two isoforms should prevent ATP uptake into mitochondria by the endogenous ANT2, leading to cell death. In contrast, the overexpression of ANT2 does not affect cell life and proliferation (Bauer *et al*., 1999; Zamora *et al*., 2004), confirming its specific role of ATP import into mitochondria in glycolytic conditions.

As shown by our results, neither *HK II* nor *ATPsynβ* were upregulated in ρ^0 cells as compared to the already transformed glycolytic parental cells. Moreover, as described in other studies (Chandel *et al*., 1998; Delsite *et al*., 2002), the expression of glycolytic genes, encoding Glut-1, aldolase A and other glycolytic proteins, was also not increased in ρ^0 cells as compared with parental cells. To confirm these results, further experiments should be done with ρ^0 cells established from partially oxidative, untransformed parental cells such as WI38 or myoblasts. However, mtDNA depletion in these oxidative cells often leads to cell death.

When human ANT proteins are compared to yeast AAC proteins, the yeast AAC3 and the human ANT2

isoforms are the most closely related, with a 53% sequence identity (Giraud *et al*., 1998). *AAC3* and ANT2 are both regulated by the similar GRBOX/ROX binding motifs. Thus, they may have the same function of ATP uptake into mitochondria (Sokolikova *et al*., 2000; Stepien *et al*., 1992). This specific ANT2 function was recently confirmed by phylogenetic studies in which the original ANT protein was from an obligate intracellular parasite, such as Rickettsia, in early eukaryotic cells (Amiri *et al*., 2003). Such endosymbionts already use a combination of two types of ATP/ADP translocase to allow switches from glycolysis (anoxia) to oxidative metabolism (normoxia).

The association of ANT2, HK II and ATPsynβ overexpression in cancer cells could be considered as an ATP import mechanism (Fig. 7): glycolytic ATP may be first transferred through porin by HK II (Bustamente *et al*., 1977) and then by ANT2 towards the matrix side of the mitochondrial inner membrane. HK II was previously shown to be the predominant overexpressed HK form in rapidly growing tumors (Mathupala *et al*., 1995) and prevents induced cell death when bound to the outer mitochondrial membrane (Pastorino *et al*., 2002). Other proteins could also be involved: creatine kinase (mitochondrial isoform), known to form complexes with ANT and VDAC (Vyssokikh and Brdiczka, 2003) and consequently could transfer imported ATP from HK II to ANT2. Unlike cytoplasmic hexokinase which can be inhibited by its glucose-6P product, HK II, bound to the external side of the mitochondrial outer membrane, is not G6P-regulated and has different kinetic parameters. This HK enzyme, irreversible in physiological conditions when unbound, could catalyze, at a particular threshold of glycolytic cytoplasmic ATP concentration, an inverse reaction leading to ATP production directly available to ANT2. The imported ATP could then be either used for essential intramitochondrial enzymatic pathways or hydrolyzed to ADP by the F1 part of ATP synthase. Different effects of OXPHOS and glycolysis inhibitors confirmed the maintenance of the $\Delta\psi$

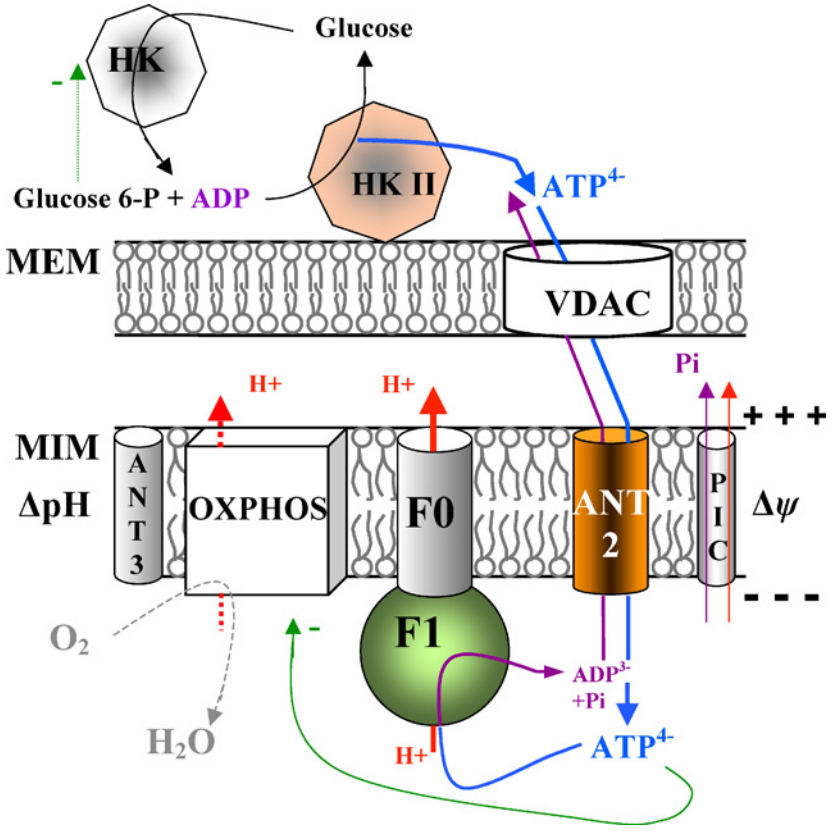

Fig. 7. A proposed mechanism for ATP uptake and OXPHOS inhibition in cancer cells. The mitochondrial HK II isoform provides ATP from glucose 6-P (G-6P) produced by the cytoplasmic hexokinase (HK). The ATP^{4-}, imported into mitochondria through the voltage-dependent anion channel (VDAC) and then by the ANT2 isoform, contributes to the maintenance of the mitochondrial membrane potential ($\Delta\psi$) and to intramitochondrial enzymatic activities.

by this ATP^{4-} import coupled to both ADP^{3-} (through ANT2) and H^+ (through ATP synthase) efflux from mitochondria. In ρ^0 cells, the proton efflux is prevented by the absence of the mtDNA-encoded subunits 6 and 8 of the F0 component of the ATP synthase, and the generation of mitochondrial $\Delta\psi$ is mainly dependent on the ATP^{4-}/ADP^{3-} exchange by the ANT2 isoform.

In conclusion, although the metabolic changes following a switch from the dual oxidative and glycolytic metabolism to an almost exclusively glycolytic metabolism may not be the key factors leading to cellular transformation and cancer, they could play a critical role in the survival and proliferation of cancer cells. Since ANT2 function contributes to the aggressiveness of cancer cells, an anti-tumor strategy targeting the *ANT2* transcript would inhibit the import of glycolytic ATP into mitochondria and provoke a decrease and possibly an arrest of cancer cell proliferation.

ACKNOWLEDGMENTS

This work was supported by the French INSERM, the University of Angers, a grant from the Collectivités Territoriales d'Angers (to A.C.). The authors thank J. Hodbert, D. Joyaux and C. Henry for technical assistance, and are grateful to Kanaya Malkani for critical reading and comments on the manuscript.

REFERENCES

Amiri, H., Karlberg, O., and Andersson, S. E. (2003). *J. Mol. Evol.* **56**, 137–150.

Balasubramanian, B., Lowry, C. V., and Zitomer, R. S. (1993). *Mol. Cell. Biol.* **13**, 6071–6078.

Barath, P., Albert-Fournier, B., Luciakova, K., and Nelson, B. D. (1999). *J. Biol. Chem.* **274**, 3378–3384.

Battini, R., Ferrari, S., Kaczmarek, L., Calabretta, B., Chen, S. T., and Baserga, R. (1987). *J. Biol. Chem.* **262**, 4355–4359.

Bauer, M. K., Schubert, A., Rocks, O., and Grimm, S. (1999). *J. Cell. Biol.* **147**, 1493–1502.

Buchet, K., and Godinot, C. (1998). *J. Biol. Chem.* **273**, 22983–22989.

Burger, C., Wick, M., Brusselbach, S., and Muller, R. (1994). *J. Cell. Sci.* **107**, 241–252.

Bustamente, E., Morris, H. P., and Pedersen, P. L. (1977). *Adv. Exp. Med. Biol.* **92**, 363–380.

Chandel, N. S., Maltepe, E., Goldwasser, E., Mathieu, C. E., Simon, M. C., and Schumacker, P. T. (1998). *Proc. Natl. Acad. Sci. U.S.A.* **95**, 11715–11720.

Cuezva, J. M., Krajewska, M., de Heredia, M. L., Krajewski, S., Santamaria, G., Kim, H., Zapata, J. M., Marusawa, H., Chamorro, M., and Reed, J. C. (2002). *Cancer Res.* **62**, 6674–6681.

Delsite, R., Kachhap, S., Anbazhagan, R., Gabrielson, E., and Singh, K. K. (2002). *Mol. Cancer* **1**, 6.

Drgon, T., Sabova, L., Nelson, N., and Kolarov, J. (1991). *FEBS Lett.* **289**, 159–162.

Duborjal, H., Beugnot, R., De Camaret, B. M., and Issartel, J. P. (2002). *Genome Res.* **12**, 1901–1909.

Faure Vigny, H., Heddi, A., Giraud, S., Chautard, D., and Stepien, G. (1996). *Mol. Carcinog.* **16**, 165–172.

Giraud, S., Bonod-Bidaud, C., Wesolowski-Louvel, M., and Stepien, G. (1998). *J. Mol. Biol.* **281**, 409–418.

Graham, B. H., Waymire, K. G., Cottrell, B., Trounce, I. A., MacGregor, G. R., and Wallace, D. C. (1997). *Nat. Genet.* **16**, 226–234.

Groen, A. K., Wanders, R. J., Westerhoff, H. V., van der Meer, R., and Tager, J. M. (1982). *J. Biol. Chem.* **257**, 2754–2757.

Houldsworth, J., and Attardi, G. (1988). *Proc. Natl. Acad. Sci. U.S.A.* **85**, 377–381.

Jouaville, L. S., Pinton, P., Bastianutto, C., Rutter, G. A., and Rizzuto, R. (1999). *Proc. Natl. Acad. Sci. U.S.A.* **96**, 13807–13812.

Kaplan, R. S. (2001). *J. Membr. Biol.* **179**, 165–183.

Kolarov, J., Kolarova, N., and Nelson, N. (1990). *J. Biol. Chem.* **265**, 12711–12716.

Kunz, W. S. (2003). *Exp. Physiol.* **88**, 149–154.

Lee, I., Bender, E., and Kadenbach, B. (2002). *Mol. Cell Biochem.* **234–235**, 63–70.

Levy, S. E., Chen, Y. S., Graham, B. H., and Wallace, D. C. (2000). *Gene* **254**, 57–66.

Liu, H., Hu, Y. P., Savaraj, N., Priebe, W., and Lampidis, T. J. (2001). *Biochemistry* **40**, 5542–5547.

Loiseau, D., Chevrollier, A., Douay, O., Vavasseur, F., Renier, G., Reynier, P., Malthiery, Y., and Stepien, G. (2002). *Exp. Cell Res.* **278**, 12–18.

Lunardi, J., and Attardi, G. (1991). *J. Biol. Chem.* **266**, 16534–16540.

Marjanovic, S., Skog, S., Heiden, T., Tribukait, B., and Nelson, B. D. (1991). *Exp. Cell Res.* **193**, 425–431.

Mathupala, S. P., Rempel, A., and Pedersen, P. L. (1995). *J. Biol. Chem.* **270**, 16918–16925.

Neckelmann, N., Li, K., Wade, R. P., Shuster, R., and Wallace, D. C. (1987). *Proc. Natl. Acad. Sci. U.S.A.* **84**, 7580-7584.

Netzker, R., Hermfisse, U., Wein, K. H., and Brand, K. (1994). *Biochim. Biophys. Acta* **1224**, 371–376.

Pastorino, J. G., Shulga, N., and Hoek, J. B. (2002). *J. Biol. Chem.* **277**, 7610–7618.

Pevny, L. H., and Lovell-Badge, R. (1997). *Curr. Opin. Genet. Dev.* **7**, 338–344.

Shepherd, D., and Garland, P. B. (1969). *Biochem. J.* **114**, 597–610.

Sokolikova, B., Sabova, L., Kissova, I., and Kolarov, J. (2000). *Biochem. J.* **352**, 893–898.

Stepien, G., Torroni, A., Chung, A., Hodge, J. A., and Wallace, D. C. (1992). *J. Biol. Chem.* **267**, 14592–14597.

Trinder, P. (1969). *J. Clin. Pathol.* **22**, 158–161.

Villani, G., Greco, M., Papa, S., and Attardi, G. (1998). *J. Biol. Chem.* **273**, 31829–31836.

Vyssokikh, M. Y., and Brdiczka, D. (2003). *Acta Biochim. Pol.* **50**, 389–404.

Warburg, O. (1956). *Science* **123**, 309–314.

Zaid, A., Li, R., Luciakova, K., Barath, P., Nery, S., and Nelson, B. D. (1999). *J. Bioenerg. Biomembr.* **31**, 129–135.

Zamora, M., Granell, M., Mampel, T., and Vinas, O. (2004). *FEBS Lett.* **563**, 155–160.